Design and Analysis of Grid Integrated Wind Energy Conversion System-Adaptive Moth Flame Optimization with ANN Technique

P.Sebastian Vindro Jude[1], Dr.R.Mahalakasmi[2]
[1] Assistant Professor/EEE, Sri Ramakrishna Engineering College, vindro@rediffmail.com
[2] Professor/, EEE Kumaraguru College of Technology, mahalakshmi.r.eee@kct.ac.in

Abstract: In the paper, adaptive technique is proposed for improving performance of the grid integrated WECS. The adaptive technique is the combination of Moth Flame Optimization (MFO) Algorithm and Artificial Neural Network (ANN) technique. The proposed method is utilized to analyze the dc link voltage and the grid side performances. Here, a cascaded H-bridge Multilevel Inverter is proposed to analyze the grid side variations and control the dynamic performances of the system. For the optimal pulses of cascaded MLI, the proposed adaptive MFO-ANN technique is developed and voltage, power regulation is achieved. The need of optimal switching operation is to avoid the complexity of the error voltage category. In the controller part, MFO algorithm is utilized to optimize the gain parameters of PID controller after that, ANN is utilized with the optimized gain values. After that, the optimal control pulse is generated to enhance the performance of grid integrated power system. The proposed adaptive MFO with ANN technique is implemented in MATLAB/Simulink working platform and the output performance is analyzed. In order to evaluate the performance of proposed method, this is contrasted with the existing techniques such as MFO and Firefly Algorithm (FA)-ANN technique.

Keywords: Cascaded H-bridge multilevel inverter, grid, MFO, ANN, FA and voltage regulation

1. Introduction

Recent years, for a cleaner enrgy and economical energy society, the world has been turning to the alternatives of fossil fuels and wind energy conversion systems (WECSs) have been drawing attention as clean electricity source [1-3] .Wind energy is one of the fastest growing renewable energy sources is wind energy and continues to flourish each year in many countries [4]. Recently, the permanent magnet synchronous generator (PMSG) has received much attention in wind-energy application. The use of permanent magnet in the rotor of the PMSG makes it unnecessary to supply magnetizing current. Hence, for the same output, the PMSG will operate at a higher power factor because of the absence of the magnetizing current and will be more efficient than other machines. The multi-pole PMSG also improves significantly the reliability of the variable speed wind turbine by using a direct-drive train system instead of the gearbox, which also results in low cost [5-7].

Presently, variable speed wind turbine generator system (WTGS) is becoming more popular than that of fixed speed [8]. Generators are used, in general, as fixed speed wind generator due to their superior characteristics such as brushless and rugged construction, low cost, maintenance free, and operational simplicity. However, it requires large reactive power to recover the air gap flux when a short circuit fault occurs in the power system [9-11]. A wind farm consists of several wind generators connected to the transmission system through a single bus [13]. The most important technical requirements for wind farms included in most grid codes, such as active and reactive power regulation, voltage and frequency operating limits and wind farm behaviour during grid disturbances.

The most important technical requirements for wind farms included in most grid codes, such as active and reactive power regulation, voltage and frequency operating limits and wind farm behaviour during grid disturbances [14, 15]. In the PMSG wind turbine system, the generator is connected to the grid through a full scale back to back pulse width modulated (PWM) converters [18]. The risk of voltage collapse for lack of reactive power support is one of the critical issues when it comes to contingencies in the power system. Closely linked to this is the LVRT capability, which is one of the most demanding requirements that have been included in the grid codes. The LVRT requirement, although details are differing from country to country, basically demands that the wind farm remains connected to the grid for voltage dips as low as 5% retained voltage [19, 20]. In the paper, adaptive MFO-ANN technique is proposed for the enhancement of cascaded h-bridge MLI based ANN technique to get the stable output of the grid integrated power system.

2. Grid Integrated Wind Energy Conversion System

In the section, the WECS is analyzed and the mathematical modeling is described. The block diagram of the grid connected WECS is depicted in the Fig.1. It consists of the PMSG, diode bridge rectifier (DBR), Boost Converter, cascaded h-bridge MLI, filter and grid respectively. In the Fig.1, R_b is the resistance, L_b is represents the inductance and V_{dc} is the dc link voltage respectively. In the WECS, the PMSG is considered for the source side and connected to the grid. The PMSG based WECS does not require any gear or drive train system which reduces the complexity of the system and reduce overall size and cost. The PMSG generator is variable speed generator which can be operated in wide range of wind speed. The DBR is most suitable configuration for synchronous generator as they do not require magnetizing current. The DBR is used to convert the generated AC to DC in order to eliminate the harmonics produced due to linearity in wind speed. The DC voltage obtained from the DBR is connected to the boost converter to control the generated torque and to obtain maximum power. A smoothing capacitor C_{dc} is used to remove ripple in the DC voltage. The cascaded h-bridge MLI is used to generate nine level output voltage of the system. The proposed model is used to improve the performance by controlling the gain parameters of the controller and generating the optimal pulses for the cascaded h-bridge MLI. The mathematical modeling of the WECS is analyzed in the following sub section.

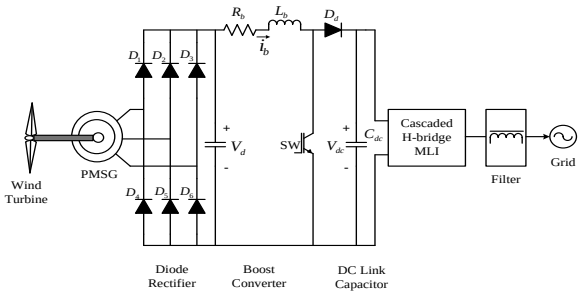

Figure 1: Structure of the WECS with MLI and proposed controller

2.1. Modeling of WECS

The main components of the proposed WECS based PMSG are the wind turbine, the PMSG (high-pole type that is manufactured for low speed applications) [26]. The wind turbine is effectively employed for the purpose of converting the wind speed into mechanical energy, which is generated by means of the wind turbine shaft of the generator. The mechanical power is appropriately defined in equation (1).

$$P_m = (0.5).\rho A C_p(u,v) V_\omega^3 \qquad (1)$$

Where, P_m represents the mechanical output power of the wind turbine, ρ , the air density (kg/m^3) , A , the area swept by blades, V_ω , the wind speed in m/s , v , the pitch angle in degree and $C_p(u,v)$, the power coefficient of the wind turbine. This power coefficient is evaluated from the equation (2).

$$C_p = 0.73\left(\frac{151}{u_i} - 0.58v - 0.002v^{2.14} - 13.2\right)e^{-18.4/u_i} \qquad (2)$$

Where, $u_i = \left(\frac{1}{\lambda - 0.002\beta} - \frac{0.003}{\beta^3 + 1}\right)^{-1}$

C_p symbolizes a non-linear function of both the Tip Speed Ratio (TSR) u and the pitch angle v. By using equation (2), the maximum power can be extracted depending on the optimum TSR value [27]. The requisite TSR may be estimated with the help of following equation (3).

$$u = \frac{\omega_r r}{V_\omega} \qquad (3)$$

Where, r corresponds to the wind turbine blade tip radius and ω_r the turbine speed. Consequently, the output mechanical torque is evaluated from the equation (4).

$$T_m = \frac{P_m}{\omega_m} \qquad (4)$$

By arranging equations (1) to (4), a simple but realistic model for the wind turbine is created to calculate T_m (Nm) and P_m (W) instantaneously

from rotor angular speed, wind speed and the pitch angle.

2.2. Modeling of PMSG

The dynamic model of the PMSG is expressed in the rotor d-q reference frame which eliminates all time varying inductances [28]. The dynamic model of the PMSG in terms of voltages and current can be described in the equations (5) and (6).

$$V_{ds} = -R_s.i_{ds} + \omega_r.L_q.i_{qs} - L_d.Pi_{ds} \quad (5)$$

$$V_{qs} = -R_s.i_{qs} - \omega_r.L_d.i_{ds} + \omega_r.u_r - L_d.Pi_{ds} \quad (6)$$

Where, V_{ds} and V_{qs} are the terminal stator voltage components (V), i_{ds} and i_{qs} are the stator current components (A), L_d and L_q are the stator inductances in the dq- reference frame (H), ω_r is the electrical generator rotational speed (rad/sec), u_r is the flux provided by the permanent magnets of the rotor, R is the stator resistance (Ω), P is the derivative operator (d/dt), d refers to the active component and q refers to the reactive component. The electromagnetic torque is calculated in the equation (7).

$$T_{em} = \left(\frac{3P}{2}\right).\left[i_{qs}.u_r - \left(L_d - L_q\right).i_{ds}.i_{qs}\right] \quad (7)$$

Finally, the electromechanical equation was formulated as equation (8).

$$T_{em} - T_e = B(\omega_m) + (J).\left(\frac{d\omega_m}{dt}\right) \quad (8)$$

Where, J is the equivalent inertia moment of the machine and turbine (kg.m^2), B is the coefficient of friction and P is the number of pole pairs. The active and reactive powers of the PMSG are calculated from the equation (9) and (10).

$$P_{pmsg} = \frac{3}{2}.\left(V_{ds}.i_{ds} + V_{qs}.i_{qs}\right) \quad (9)$$

$$Q_{pmsg} = \frac{3}{2}.\left(V_{qs}.i_{ds} + V_{ds}.i_{qs}\right) \quad (10)$$

An accurate model for permanent magnet synchronous generator was implemented using equations (5 to 10) to compute the three-phase currents of the PMSG and the rotational speed, which is used as a feedback signal to the wind turbine model, from the three-phase voltages and the mechanical torque.

3. Control Strategy analysis of MFO-ANN Technique

In the section, the control strategy of grid connected WECS is described and analyzed the dynamic characteristics of the proposed method. In the previous section, the modeling part of the proposed system is described. In the paper, the WECS is utilized to analyze the power flow of the grid system. With the utilization of WECS, the cost and pollution is cheap and free. The power is transferred from the WECS to grid, it is passed through the DBR. The rectifier has been used to convert the power from AC to DC. After that, the dc power is achieved and it is to be maximized by using the boost converter. Then the maximum power is transferred to the cascaded h-bridge MLI and converted into the nine level sources. It is synchronized with the grid, it is achieved by the enhancement of the controller parts. Moreover, the cascaded h-bridge MLI performance is also enhanced and the optimum pulses are generated. For the power flow analysis, the real power, reactive power, voltage regulation and THD are evaluated. Therefore, the control system consists of power and voltage regulations blocks, which are analyzed with the help of the proposed controller. The control structure of the proposed method is illustrated in the Fig.4. The detailed analysis of the proposed control topology is described with the following section.

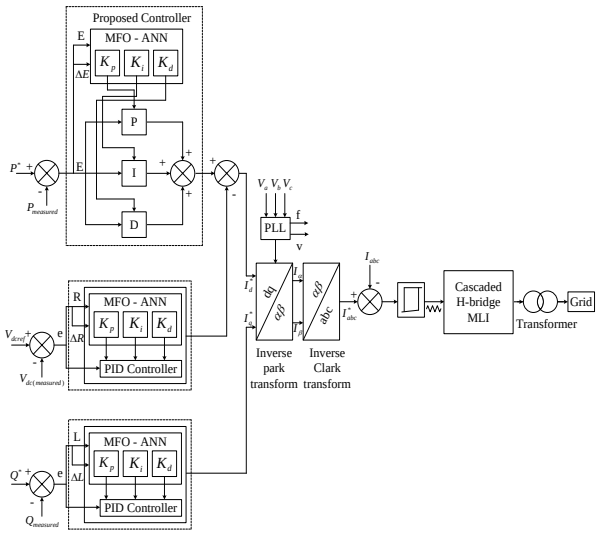

Figure 4: Proposed controller with PID controller

3.1. Power and Voltage Control loops

Generally, each control strategy has its own distinct parameters a specific task. In power control strategy, the real power (P_m) is measured by utilizing the PLL method and compared with the reference power (P^*). After that, the error values are determined and mentioned as the factor as (E). The power control loop is fed through MFO-ANN technique for optimizing the gain parameters of the controller. Here, the PID controller is utilized to analyze the real power of the proposed system. Initially, the error value of power is given to the input of the PID controller and the corresponding gain parameters are tuned optimally. For the optimal tuning process, the MFO-ANN technique is applied. In the MFO, the gain parameters K_p, K_i and K_d are randomly generated and the error values are considered as the input. Based on that, the optimal gain parameters and corresponding inputs are evaluated. The optimized gain parameters are given to the input of PID controller. After that, the PID controller is tuned optimally and produces the optimal control pulses. Similarly, the other blocks are worked and analyzed their performances. Based on the three blocks, the control pulses of cascaded h-bridge MLI is generated and analyzed the dynamic characteristics. For connecting WECS to grid, the optimal pulses of cascaded h-bridge MLI is analyzed [32]. The d-axis and q-axis current components of the inverters are used to control instantaneous reactive and active power exchange between the DC-link voltage and the grid. The output voltage of inverter is a square wave of high frequency. Fig.4. shows that, the synchronous reference frame of the control variables converted into dc quantities. Thus the grid side converter was controlling and filtering can be done easily. Another advantage is that the PID regulator gives an improved performance while regulating dc variables. After that, the PLL is utilized to obtain the grid angle for the transformation process.

A Phase Locked Loop (PLL) is used to obtain grid angle θ for grid synchronization and coordinate transformation. This control strategy guarantees fast transient response and high static performance due to internal control loops [33]. Grid currents are decomposed into d and q-axis currents to provide separate control for active and reactive power. Such controlling helps to attain high power factor and sinusoidal grid currents. The active and reactive power produced by wind energy conversion system is calculated using equations (15) and (16).

$$P = \frac{3}{2}\left(E^d.i^d + e^q.i^q\right) + \left(R^d.i^d + R^q.i^q\right) + \left(L^d.i^d + L^q.i^q\right) \quad (15)$$

$$Q = \frac{3}{2}\left(E^d.i^d - e^q.i^q\right) + \left(R^d.i^d - R^q.i^q\right) + \left(L^d.i^d - L^q.i^q\right) \quad (16)$$

The d-axis of synchronous reference frame has aligned absolutely on the grid voltage vector E^q, R^q and L^q. In equation (17) and (18) indicates clearly that active power is proportional to direct axis i^d and the reactive power is proportional to quadrature axis current i^q.

$$P = \frac{3}{2}\left(E^d.i^d\right).\left(R^d.i^d\right).\left(L^d.i^d\right) \quad (17)$$

$$Q = -\frac{3}{2}\left(E^d.i^q\right).\left(R^d.i^q\right).\left(L^d.i^q\right) \quad (18)$$

The d-axis reference is usually obtained from DC-link voltage controller. The inverse park transform is get the input of I_d^* and I_q^* and these are converted by the output is i_α and i_β. The inverse Clark transform is used to convert the two phase output into three phase output is i_{abc}. Then the three phase actual current is compared with the reference current and generating the optimal pulses for the controlled cascaded h-bridge MLI converter. To enhance the performance of cascaded h-bridge MLI converter in

both control loops, the optimal gain parameter is determined. Moreover, the measured values are determined from the PLL loops. In order to operate under synchronization with grid, the proposed system uses three PID controllers. The q-axis reference can be set to zero to get unity power factor. In proposed system is used to generate switching pulses to inverter because of fine dynamic response. The PLL keeps source parameters unaffected from grid harmonics, phase shifts or voltage sags. An LC filter is used between inverter and grid to minimize the harmonics and to improve power quality of the WECS in addition to control strategy. The adaptive technique has been briefly explained in the below section 4.2.

3.2. Moth Flame Optimization Algorithm and ANN for grid connected WECS

In this proposed scheme, adaptive technique has performed for controlling the optimal gain parameter and generates the optimal pulses for cascaded h-bridge MLI. In the controller process, the MFO algorithm is utilized to optimize the control gain parameters. In the paper, the MFO algorithm is developed for the optimization of the voltage and power blocks. For the controllers, the gain parameters are randomly generated and the power, voltages are considered as the input of the proposed algorithm. The objective function of the algorithm is to minimize the error signals of power and voltage regulation blocks. After that, the corresponding gain parameters are formed as a dataset. The output of MFO algorithm is given as the input of the ANN technique. In the ANN process, the gain and error values are trained and achieve the optimal results for the PID controllers. Based on the controller output, the transformations algorithms are worked done and generated the optimal pulses of cascaded h-bridge MLI. The detailed analysis of the proposed MFO algorithm is explained as below,

3.2.1. General Behaviors of MFO algorithm

Moth-Flame Optimization (MFO) is natural inspired optimization algorithm proposed by Mirjalili. MFO gets its inspiration from transverse orientation of moths in nature. The MFO is one of the newest swarm intelligence optimization techniques. The MFO algorithm vividly simulates the behavior of moths, which at nighttime navigate around flames using a mechanism called transverse orientation [34]. According to this paper, MFO algorithm is utilized for optimize the multi objective functions. Here the error values are given to the input of the each proposed system. In addition the considered objective function of fitness function is minimized. By minimizing the fitness function by get the optimal parameters of PID controllers. Moreover the proposed MFO algorithm stepwise procedure is presented below.

Step 1: Process of parameters Initialization

Initially, the PID controller parameters are initiated randomly such as, K_P , K_I and K_D respectively. The primary parameters of MFO includes, randomly generate initial population for moths and flames with dimensions, the number of variables, the maximum iteration number. Specify the random generation of upper bound and lower bound of each variable as follow,

Lower bound: $\alpha = \alpha_1, \alpha_2, \alpha_3, ..., \alpha_{n-1}, \alpha_n$ (19)

Upper bound: $\beta = \beta_1, \beta_2, \beta_3, ..., \beta_{n-1}, \beta_n$ (20)

Step 2: Position initialization process

The MFO makes an improved trade-off between exploration and exploitation of the search space using a specific flame which is assigned to each moth. In order to model the spiral of the moths, a matrix was used to represent a set of n moths. Each moth and flame can fly in different dimensions in space by setting number of variables for each moth and flame. Here the position of the moths and flames are indicated as equations (21) and (22) respectively.

$$M = \begin{bmatrix} m^{1,1} & \cdots & m^{1,d} \\ \vdots & \ddots & \vdots \\ m^{n,1} & \cdots & m^{n,d} \end{bmatrix} \quad (21)$$

$$F = \begin{bmatrix} f^{1,1} & \cdots & f^{1,d} \\ \vdots & \ddots & \vdots \\ f^{n,1} & \vdots & f^{n,d} \end{bmatrix} \quad (22)$$

Where, n is the number of moths and d is the number of dimensions. And the initialization of moth and flame can be calculated by,

$$M_d^x or\ F_d^x = rand(\beta_d - \alpha_d) + \alpha_d \quad (23)$$

Where, M_d^x and F_d^x denoted as the number of variables or dimensions, $rand$ is represents the random number generated with uniform distribution in the interval [0, 1], α_d and β_d denotes the lower and upper bounder of d^{th} variables respectively.

Step 3: Evaluation of fitness function

Each moth and flame is evaluated by passing the corresponding position vector to the desired objective function which then assigns to a column vector OM and OF the best fitness value of each moth and flame.

$$OM = \begin{bmatrix} OM^1 \\ \vdots \\ OM^n \end{bmatrix} \quad (24)$$

$$OF = \begin{bmatrix} OF^1 \\ \vdots \\ OF^n \end{bmatrix} \quad (25)$$

Based on the above function, the best fitness function is evaluated by the equation shown as follow.

$$FF = Min\left[E(t)\right] \quad (26)$$

Where, the mean of fitness function (FF) is minimize the error value of $\left[E(t)\right]$ in cascaded h-bridge MLI based on the grid integrated WECS.

Step 4: Process of start iteration

In this function the moth moves around the solution space. In order to mathematically model the behavior of converging towards the light or moon, a logarithmic spiral is defined for the MFO algorithm to simulate the spiral flying path of moths with respect to a flame. The presented MFO algorithm by using logarithmic spiral function as follow,

$$M^i = S\left(M^i, F^j\right) \quad (27)$$

$$S\left(M^i, F^j\right) = D^i.e^{bt}.\cos(2\pi t) + F^j \quad (28)$$

Where

$$D^i = \left|F^j - M^i\right| \quad (29)$$

Where, S is the spiral function, M^i is the i[th] moth, F^i indicates j[th] flame, D^i means the distance between the ith moth and j[th] flame, b is a constant in order to define the spiral function and t is derived randomly between – 1 and 1. The spiral equation is the key component of the MFO algorithm because it describes how the moths update their positions around the flames but not necessarily in the space between them.

Step 5: The optimal result selection process

The position of objective flame would be updated if any of the moths becomes fitter than it. According to this rule, the position and the fitness of flames would be updated, and then re-determine the best result and update its position if any moth becomes fitter than the best flame selected from the previous iteration. When the iteration criterion is reach, the best solution would be returned as the best obtained approximation of the optimum.

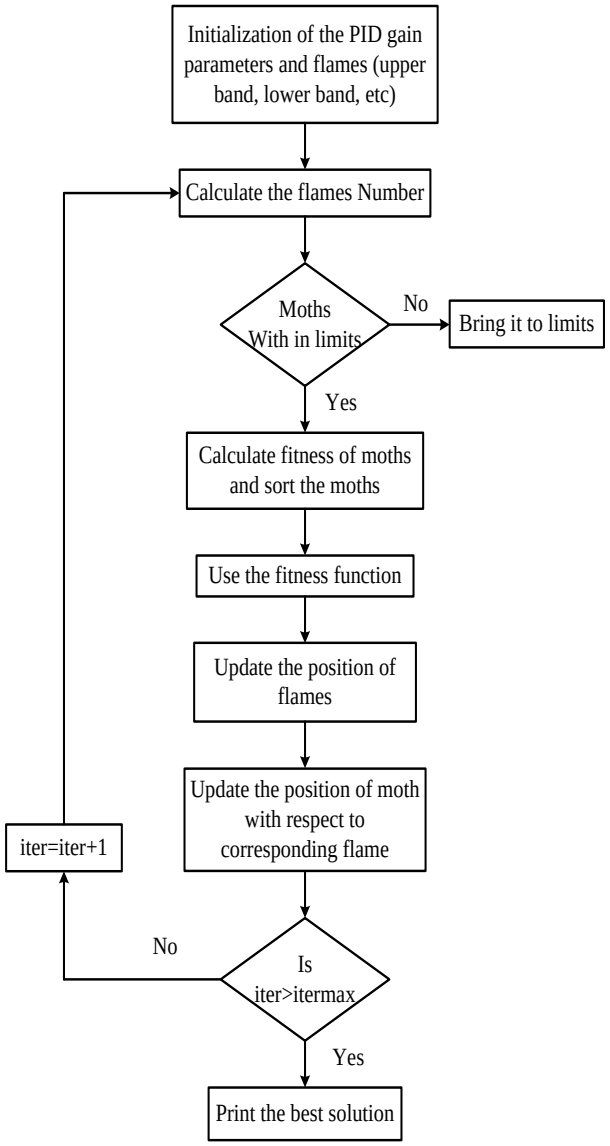

Figure 5: Flow chart for MFO algorithm

The general flowchart of MFO algorithm is illustrated in figure 5. Then the resultant value of MFO algorithm is optimized by using the proposed ANN technique. Moreover, the performance of ANN technique is investigated in below sub section 4.2.2.

3.2.2. Analysis of ANN technique

ANN is a mathematical model that performs a computational simulation of the behavior of neuron in the human brain by replicating the brain's pattern to produce results based on the learning of set of training data. As seen in figure 6, the inputs of ANN controller are the error value $(E(t))$. The output of the ANN is given to the input of PID controller which is considered as the Y_1, Y_2 and Y_3. In order to achieve the efficient control of the system, the neural network should be trained in such a way that for the given input of the controller should produce a proper gain signals. The detailed description of the ANN is included in this section. The multi layer feedforward network with a back-propagation learning algorithm is one of the most popular neural network architectures [35]. Typically, a neural network consists of three layers such as input layer, output layer and intermediate or hidden layer. The training structure of ANN is illustrated in Fig. 6. Back propagation algorithm is used to train the neural networks.

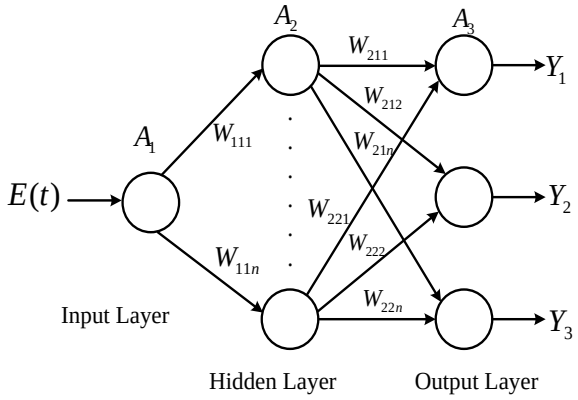

Figure 6: Training structure of ANN using proposed adaptive approach

Here, the weight of the network is assigned for input layer to hidden layer and hidden layer to output layer. From the input layer to hidden layer weights are denoted as $(W_{111},...W_{11n})$ respectively. The hidden layer to output layers weights are represented as $(W_{211},W_{212},...W_{21n})$ and $(W_{221},W_{222},...W_{22n})$. The output of the node is specified as Y_1, Y_2 and Y_3. Then the neural network is trained by back propagation algorithm. The training algorithm steps are described as follows,

Steps for Training algorithm

Step 1: Here, the weight of each neuron is assigned randomly for learning the network. The minimum and maximum weight (i.e., $W=(W_{\min},W_{\max})$) of the interval range is specified as $(0,1)$.

Step 2: Using the following equation, the back propagation error of the network is calculated.

$$error(BP) = Y(t\arg et) - Y(out) \quad (30)$$

Where, $Y(t\arg et)$ is the network target of the node and $Y(out)$ is the current output of the network.

Step 4: From the neural network, the current output is determined by following them,

$$Y(out) = \sum_{n=1}^{N} w_{2n} Y_i(n) + \beta \quad (31)$$

Here, w_{ij} is the weight of the $i-j$ link of the network. Then, Y_i is the output of i^{th} hidden neuron. Also, find out the change in weights based on the obtained BP error.

Step 5: Determine the bias (or) activation function of the network.

$$Y_i(n) = \frac{1}{1+\exp(-w_{1n} * Y_i(n))} \quad (32)$$

Step 6: The new weights of the each neurons of the network are updated by using the following equation,

$$new(w) = prev(W) + \Delta W \quad (33)$$

Here, $new(w)$ is the new weight, $prev(w)$ is the previous weight and Δw is the change of weight of each output.

Step 7: Using the following equation, change of weight in the network is evaluated.

$$\Delta w = \delta . Y_{out} . error(BP) \quad (34)$$

In Equation. (34), δ is the learning rate. Repeat the above steps till the $error(BP)$ gets minimized $error(BP) < 0.1$. Once the neural network training process is completed, the network is trained well for minimizing the error value of the input. Then the neural network output is given to the input of the PID controller. After that, the gain parameter of PID controller is optimized. From the two phase analysis, the voltage, real and reactive power is controlled optimally using the proposed method. Based on the controller output, the optimal pulses of cascaded h-bridge MLI is generated. The detailed experimental results analysis was given by the following section 5.

4. Results and Discussions

In this section, the performance analysis of proposed adaptive technique is analyzed with the grid integrated WECS. It describes the cascaded h-bride MLI of the grid integrated power system. Here the operating performance of the proposed controller is implemented in the MATLAB/Simulink platform. The effectiveness of the proposed control method is analyzed and compared with the traditional approaches such as MFO and FA-ANN. The Simulink diagram of the proposed system with the grid integrated WECS is demonstrated in the diagram 7, which is used to control the power flow of the grid integrated WECS with the help of proposed adaptive technique. In the operation, the PID controller is employed to switch the real, reactive power and voltage of the grid integrated WECS. The implementation parameters are analyzed and illustrated in the table 2.

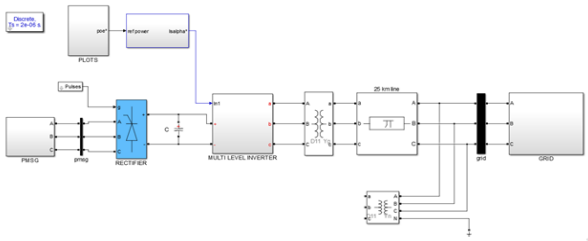

Figure 7: Matlab/Simulink model of the proposed method with cascaded H-bridge multilevel inverter

Description of parameters	Values
Rated wind speed	$12(m/s)$
Base rotational speed	1.2 (p.u)
Nominal mechanical output power	605.142 (W)
Stator phase resistance	0.18 (ohm)
Armature inductance	$0.0167(H)$
Pole pairs	4
Rotor type	Round
Flux linkage	$0.0714(V_s)$
Torque constant	$0.4286(N_m)$
Inertia	$0.00062\ J(kgm^{-2})$
Friction factor	$0.00030\ F(Nms\ )$

Table 2: Implementation parameters of the proposed method

4.1. Performance analysis

In the sub section, the performance of the proposed controller is analyzed and tested. The propose technique is utilized to regulate the dc link voltage and cascaded h-bridge MLI according to their control signals. The performance of the proposed controller is analyzed in the normal wind speed condition and varied wind speed condition. These analyses of the two conditions are formed as the different types of cases such as case 1 and case 2 respectively. The analyzed outputs of the proposed method are compared with MFO method and FA-ANN methods. The detailed analysis of the proposed method is described in the following section.

Case 1: Analysis of normal wind speed

Case 2: Analysis of varied wind speed

Analysis of Case 1

At first, the execution of rotor speed and wind speed are analyzed in the ordinary condition and outlined in figures 8. Although the proposed technique, the controllable region of pitch angle is between rated wind speed (12.5 m/s) and the cut-out wind speed (24 m/s). If the wind speed is smaller than the rated speed, then the proposed control technique is employed. While if the wind speed is larger than the rated speed, then the output power of the PMSG is smoothed by the pitch angle control.

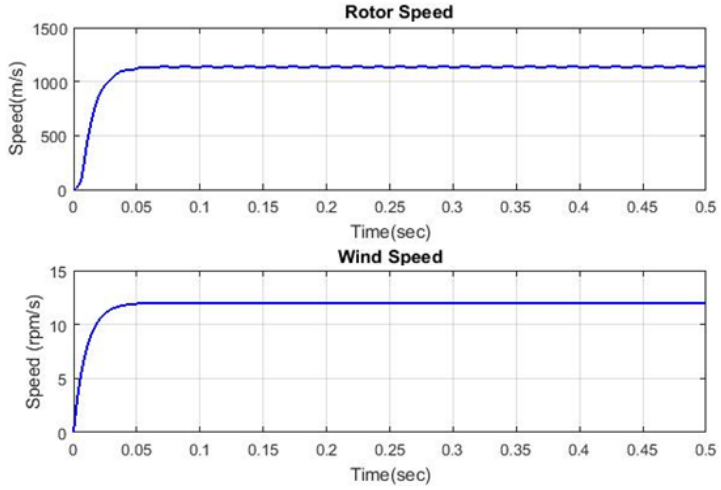

Figure 8: Performance analysis of normal condition with rotor speed and wind speed

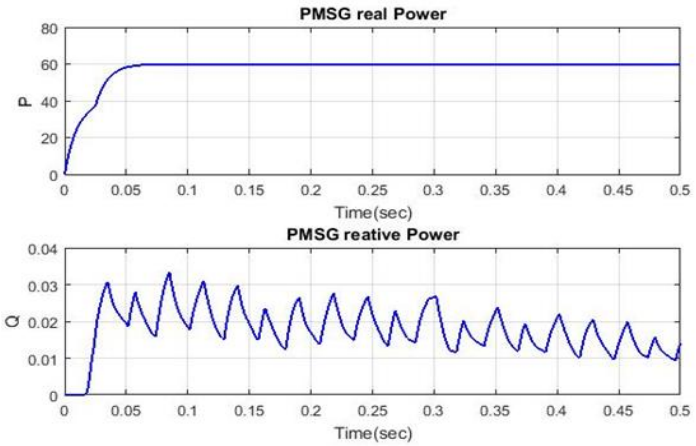

Figure 9: Performance of active power and reactive power in the PMSG

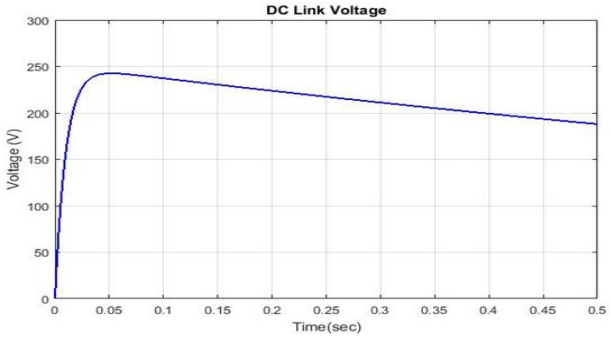

Figure 10: Performance of dc-link voltage at normal operation

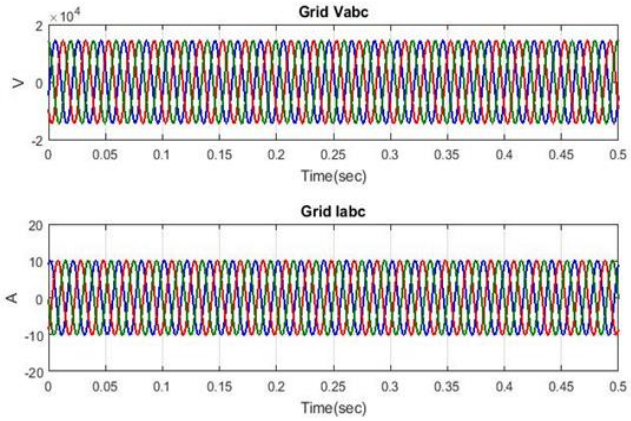

Figure 11: Performance analysis of normal condition with three phase voltage and current of grid

In the figure 8 shows that, the performance of the normal condition for analyzing the rotor speed and wind speed. The rotor speed and wind speed is modeled by a random function. In the figure 9 illustrates, the active and reactive powers of the PMSG has been represented. Here the electrical speed of the PMSG is controlled according to the optimum rational speed at the time wind speed. The active power and reactive powers of PMSG is takes settling process at 0.458 seconds. In the figure 10 shows that, the steady state output of dc-link voltage at normal condition has been illustrated. The dc voltage is takes settling time is 0.5 seconds at corresponding voltage is 190V respectively. In the figure 11 shows that. The performance analysis of the three phase voltage and current of grid at normal condition has been illustrated.

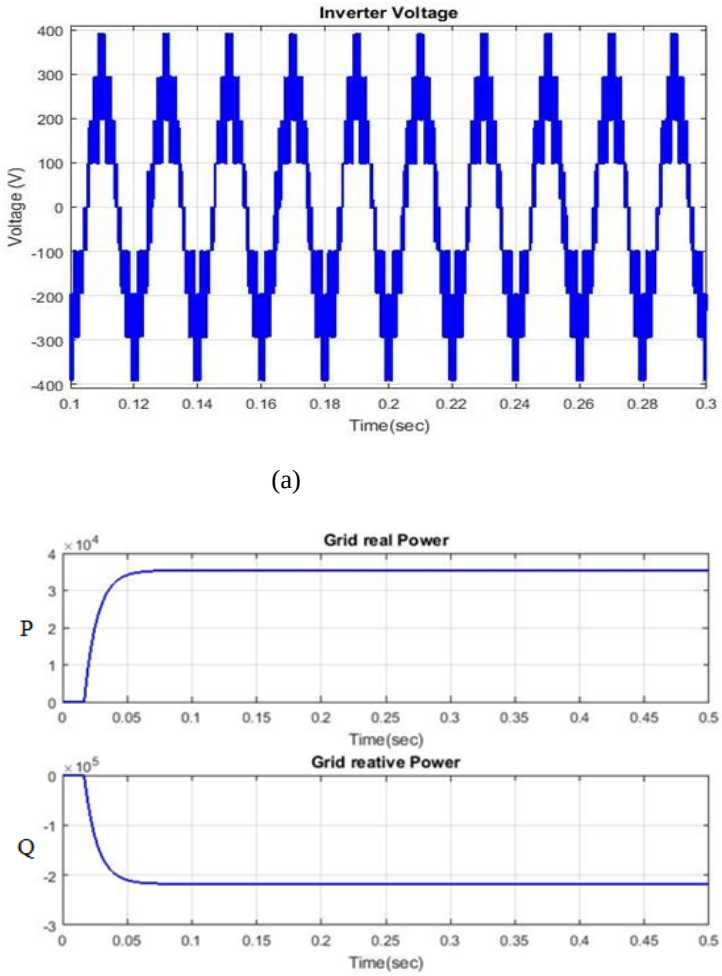

Figure 12: Performance analysis of (a) inverter voltage and (b) grid real and reactive power

In the figure 12 (a and b) shows that, the performance analysis of inverter voltage, grid real and reactive power respectively. From these figures, it is seen that the grid side voltage is kept at the rated value and the active power. It is confirmed that a simple and stable output power smoothing with more flexibility and the reduction of the wind turbine blade stress is achieved by using the proposed control technique. The variations in the power are mostly stabilized using the proposed control technique. But for grid integration the grid code must be followed thus in order to reduce the fluctuation the VOC strategy is used.

Analysis of Case 2

Here, the voltages are analyzed in the various speed conditions. Utilizing the proposed controller based cascaded h-bridge MLI the active power, reactive

power, dc-link voltage and harmonic compensation performance are analyzed. The proposed model is tested with varying wind speed as shown in figure 13. The power and voltages associated with the wind generator changes according to input wind speed. Then the small change in wind speed causes a huge variation in output power, thus increasing the voltage fluctuation for grid compliance.

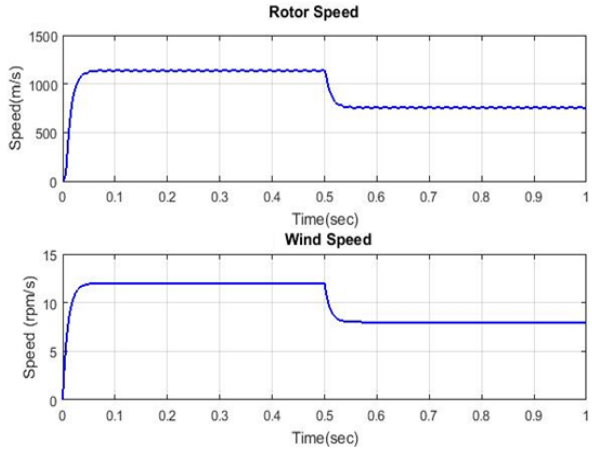

Figure 13: Performance analysis of various speeds of rotor and wind

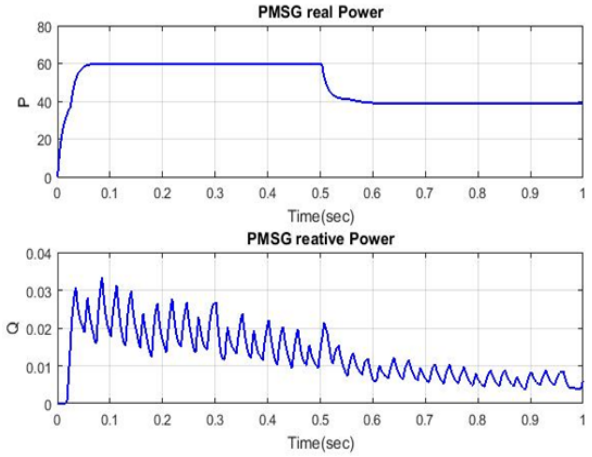

Figure 14: Performance of active power and reactive power in the PMSG

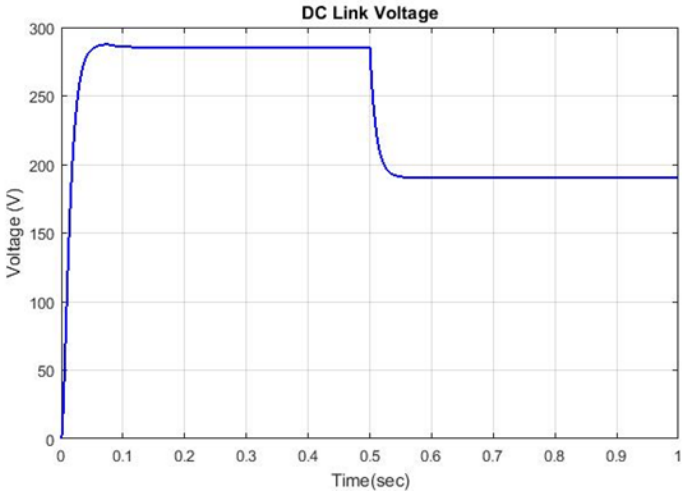

Figure 15: Performance of dc-link voltage at various operations

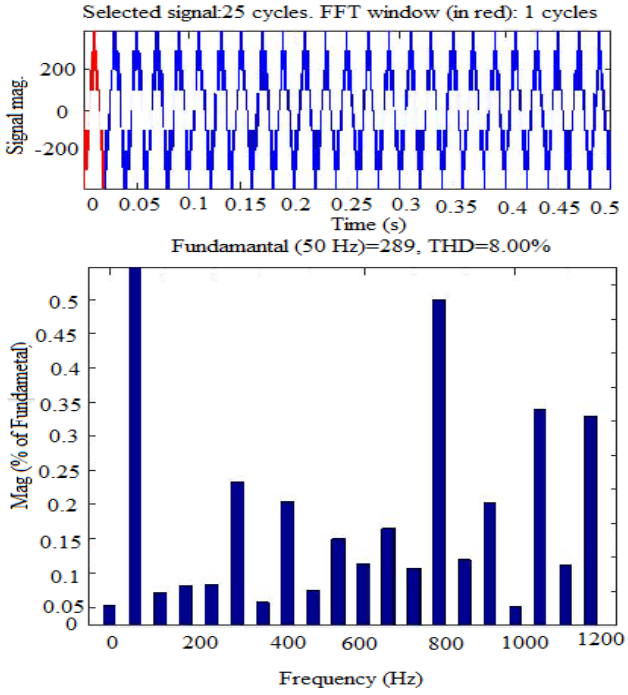

Figure 16: THD analysis of proposed method

From the figure 14 shows that, the performance of the PMSG real and reactive power using the proposed technique has been illustrated. In the figure 15 shows, the dc-link voltage of the proposed system has been analyzed. Here the dc-link rise time is 0.001 second, peak overshoot time is 0.05 seconds and steady state reach the 0.55 seconds i.e., settling process at corresponding voltage is 190V respectively. In the figure 16 shows that for the

output THD analysis of proposed method output has been illustrated. The THD is 8% for the output of proposed control technique of the grid integrated power system. From the results, it is determined that the co-ordinate control strategy is the suitable solution to extract the maximum power from the available wind and reduce the harmonic in the grid integrated power system. The proposed control technique is efficient technique the non-linearity of the power system and better stability of grid voltage and power. The comparison of proposed technique and existing methods has been detailed explained in the sub section 5.2.

4.2. Comparison analysis

In the comparison investigation, the two cases are analyzed and performed the dc link voltage regulations. At that point, the settling time, overshoot time and rising times are analyzed. From the above case, settling time, peak overshoot time and undershoot time are analyzed. In the comparison graphs figure 17 (a), the proposed technique gives closest voltage value to optimal value and moves constantly. But for the existing method, the voltage values are very far from the optimal one and which cannot be feasible for offering better voltage. In the figure 17 (b) shows that, the peak overshoot time is the proposed, MFO method and FA-ANN technique are t= 0.05 seconds, t= 0.055 seconds and t= 0.06 seconds respectively. Similarly, the settling time is proposed, MFO method and FA-ANN technique are 0.55 seconds at corresponding 190 V, 0.56 seconds at corresponding 195 V and 0.57 seconds at corresponding 205 V analyzed which is respectively. This assessment shows that the proposed method is the finest method to incredulous the nonlinearity in this power system with great reliability, more robust and good performance than the other approaches as can be explained in the figure 17.

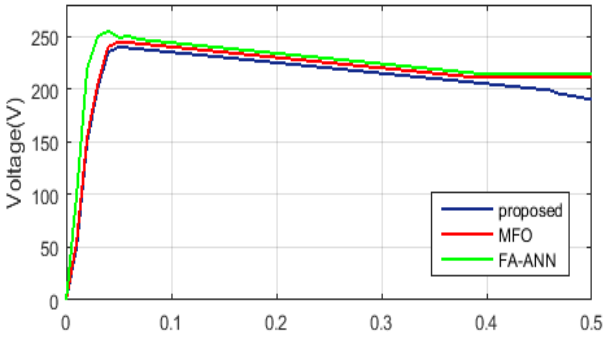

(a)

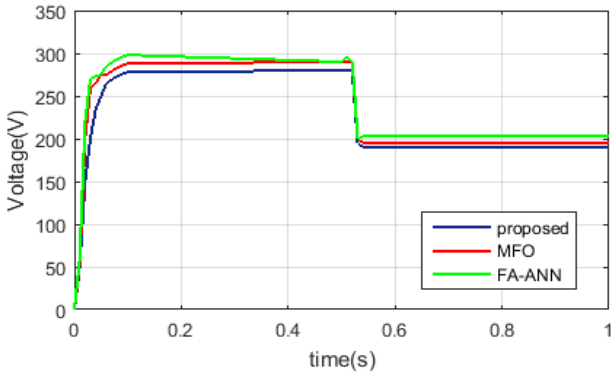

(b)

Figure 17: Comparison analysis of dc voltages in (a) case-1 and (b) case-2

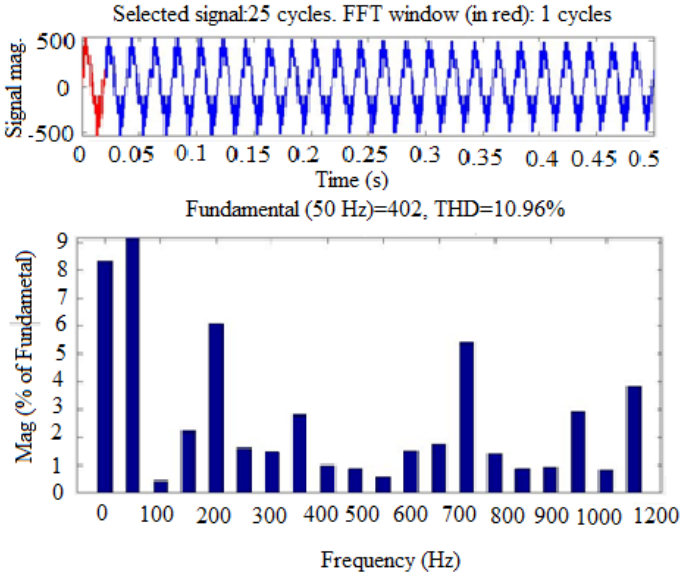

Figure 18: THD analysis of MFO method

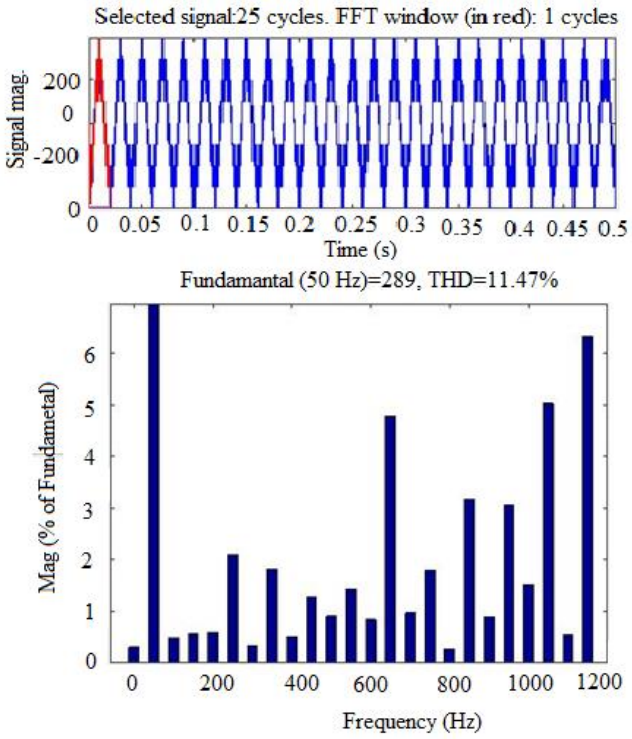

Figure 19: THD analysis of FA-ANN method

THD %	Existing methods			Proposed method
	PSO [36]	FA-ANN	MFO	MFO-ANN
	9.755	11.47	10.96	8.00

Table.3: Comparison of %THD of existing and proposed method

The above figure 18 and 17 shows that, the comparison analysis of THD in existing methods such as MFO and FA-ANN has been illustrated. The proposed and existing methods such as, PSO, FA-ANN, MFO and proposed technique are presented and the values are arranged in table 3. It shows, the proposed technique have very less percentage of harmonics to other control methods. The minimum THD of proposed controller is 8.00% respectively.

5. Conclusion

In the paper, the adaptive MFO-ANN technique was proposed to analyze the grid connected WECS. Here, the cascaded h-bridge MLI was designed for getting the optimal results. For the controller designing process, the voltage, real and reactive power blocks are analyzed with the help of the proposed method. Initially, the voltage control blocks are analyzed and determine the optimal pulses for the cascaded h-bridge MLI. Here, the error voltage was determined and regulated the voltage using the adaptive MFO-ANN technique. For the analysis process, the PID controller was tuned and minimized the corresponding error functions. The proposed MFO-ANN based grid connected WECS was implemented in Matlab/Simulink platform. The proposed technique was utilized for controlling and analyzing the power flow of the grid integrated WECS. The performances of the proposed method was demonstrated and contrasted with the existing techniques such as MFO and FA-ANN technique. The dynamic behavior of the grid integrated WECS was analyzed such as wind speed, grid speed, active and reactive power of grid side inverter, THD and etc. Based on the analysis of the proposed technique is superior to the other techniques. From the results analysis, justified that the proposed technique has a minimization of switching losses and THD which is competent over the other techniques. From the obtained result, the proposed adaptive MFO-ANN based PID controller give better solution for grid integrated WECS by minimizing the THD. In addition, the settling time was also analyzed and provides better voltage profile due to its robust exploitation capability than the exiting techniques. With optimized design parameters, the grid integrated power system design attained a THD of 8.00% which is a significant improvement considering the simplicity of this method.

References

[1] Hua Geng, Geng Yang, Dewei (David) Xu and Bin Wu, "Unified Power Control for PMSG-Based WECS Operating Under Different Grid Conditions", IEEE Transactions On Energy Conversion, Vol.26, No.3, pp.822-830, 2011

[2] Akie Uehara, Alok Pratap, Tomonori Goya, Tomonobu Senjyu, Atsushi Yona, Naomitsu Urasaki and Toshihisa Funabashi, "A Coordinated Control Method to Smooth Wind Power Fluctuations of a PMSG-Based WECS", IEEE Transactions On Energy Conversion, Vol.26, No.2, pp.550-558, 2011

[3] Francisco Huerta, Ronald L.Tello and Milan Prodanovic, "Real-Time Power Hardware-In-The-Loop Implementation of Variable-Speed Wind Turbines", IEEE Transactions on Industrial Electronics, Vol.64, No.3, pp.1893-1904, 2017

[4] Venkata Yaramasu, Apparao Dekka, Mario J.Duran, SamirKouro and BinWu, "PMSG-based wind energy conversion systems: survey on power

converters and controls", IET Transactions on Electric Power Applications, Vol.11, No.6, pp.956-968, 2017
[5] Fujin Deng, Dong Liu, Zhe Chen and Peng Su, "Control Strategy of Wind Turbine Based on Permanent Magnet Synchronous Generator and Energy Storage for Stand-Alone Systems", An International Journal of Electrical Engineering, Vol.3, No.1, pp.51-62, 2017
[6] Shao Zhang, King-Jet Tseng, D.Mahinda Vilathgamuwa, Trong Duy Nguyen and Xiao-Yu Wang, "Design of a Robust Grid Interface System for PMSG-Based Wind Turbine Generators", IEEE Transactions On Industrial Electronics,Vol.58, No.1, pp.316-328, 2011
[7] Omid Alizadeh, Amirnaser Yazdani, "A Strategy for Real Power Control in a Direct-Drive PMSG-Based Wind Energy Conversion System", IEEE Transactions On Power Delivery, Vol.28, No.3, pp.1297-1305, 2013
[8] Yinru Bai, Baoquan Kou and C.C.Chan, "A Simple Structure Passive MPPT Stand-alone Wind Turbine Generator System", IEEE Transactions on Magnetics, Vol.51, No.11, pp.1-4, 2015
[9] Venkata Yaramasu, Apparao Dekka, Mario J.Duran, Samir Kouro and Bin Wu, "PMSG-based wind energy conversion systems: survey on power converters and controls", IET Transactions on Electric Power Applications, Vol.11, No.6, pp.956-968, 2017
[10] Hua Geng,Xinze X and Geng Yang, "Small-signal stability of power system integrated with ancillary-controlled large scale DFIG-based wind farm", IET Renewable Power Generation,Vol.11, No.8, pp.1191-1197, 2016
[11] Z.Zhang, F.Wang, J.Wang, J.Rodriguez and R.Kennel, "Nonlinear Direct Control for Three-Level NPC Back-to-Back Converter PMSG Wind Turbine Systems: Experimental Assessment With FPGA", IEEE Transactions on Industrial Informatics, Vol.13, No.3, pp.1172-1183, 2017
[12] Daniel J.Trudnowski, Andrew Gentile, Jawad M.Khan and Eric M.Petritz, "Fixed-Speed Wind-Generator and Wind-Park Modeling for Transient Stability Studies", IEEE Transactions on Power Systems ,Vol.19, No.4, pp.1911-1917, 2004
[13] M.Tsili and S.Papathanassiou, "A review of grid code technical requirements for wind farms" IET Transactions On Renewable Power Generation,Vol.3, No.3, pp308-332, 2009
[14] Graham Pannell, David J.Atkinson, and Bashar Zahawi, "Minimum-Threshold Crowbar for a Fault-Ride-Through Grid-Code-Compliant DFIG Wind Turbine", IEEE Transactions On Energy Conversion, Vol.25, No.3, pp.750-759, 2010
[15] S.M.Muyeen, Rion Takahashi, Toshiaki Murata, and Junji Tamura, "A Variable Speed Wind Turbine Control Strategy to Meet Wind Farm Grid Code Requirements", IEEE Transactions On Power Systems, Vol.25, No.1, pp.331-340, 2010
[16] Marta Molinas, Jon Are Suul and Tore Undeland, "Low Voltage Ride Through of Wind Farms With Cage Generators: STATCOM Versus SVC", IEEE Transactions On Power Electronics, Vol.23, No.3, pp.1104-1117, 2008
[17] Harag Margossian,Geert Deconinck and Juergen Sachau, "Distribution network protection considering grid code requirements for distributed generation", IET Transactions On Generation, Transmission and Distribution,Vol.9, No.12, pp.1377-1381, 2015
[18] Fengjiang Wu, Xiaoguang Li, Fan Feng and Hoay Beng Gooi, "Efficiency enhancement scheme of cascaded multilevel grid-connected inverter and its improvement to eliminate effect of non-ideal grid conditions", An International Journal of Electrical Power and Energy Systems, Vol.76, pp.120–128, 2016
[19] Y.V.Pavan Kumar and Bhimasingu Ravikumar, "A simple modular multilevel inverter topology for the power quality improvement in renewable energy based green building microgrids", An International Journal of Electric Power Systems Research, Vol.140, pp.147-161, 2016
[20] Giraja Shankar Chaurasia, Amresh Kumar Singh, Sanjay Agrawal and N.K.Sharma, "A meta-heuristic firefly algorithm based smart control strategy and analysis of a grid connected hybrid photovoltaic/wind distributed generation system", An International Journal of Solar Energy, Vol.150, pp.265–274, 2017
[21] Naggar H.Saad, Ahmed A.El-Sattar and Mohamed E.Marei, "Improved bacterial foraging optimization for grid connected wind energy conversion system based PMSG with matrix converter", Ain Shams Engineering Journal, 2017
[22] Mohsen Rahimi, "Modeling, control and stability analysis of grid connected PMSG based wind turbine assisted with diode rectifier and boost converter", An International Journal of Electrical Power and Energy Systems, Vol.93, pp.84–96, 2017
[23] F.D. Bianchi, R.J. Mantz and C.F. Christiansen, "Gain scheduling control of variable-speed wind energy conversion systems using quasi-LPV models", An International Journal of Control Engineering Practice, Vol.13, pp.247-255, 2005
[27] Saad, Naggar H., Ahmed A. El-Sattar, and Mohamed E. Marei, "Improved bacterial foraging optimization for grid connected wind energy conversion system based PMSG with matrix converter", Ain Shams Engineering Journal, 2017

[28] Uehara, Akie, Alok Pratap, Tomonori Goya, Tomonobu Senjyu, Atsushi Yona, Naomitsu Urasaki, and Toshihisa Funabashi, "A coordinated control method to smooth wind power fluctuations of a PMSG-based WECS", IEEE Transactions on energy conversion, Vol.26, No.2, pp.550-558, 2011

[29] Nami, Alireza, Firuz Zare, Arindam Ghosh, and Frede Blaabjerg, "A hybrid cascade converter topology with series-connected symmetrical and asymmetrical diode-clamped H-bridge cells", IEEE Transactions on Power Electronics, Vol.26, No.1, pp.51-65, 2011

[30] Khoucha, Farid, Mouna Soumia Lagoun, Abdelaziz Kheloui, and Mohamed El Hachemi Benbouzid, "A comparison of symmetrical and asymmetrical three-phase H-bridge multilevel inverter for DTC induction motor drives", IEEE Transactions on Energy Conversion, Vol.26, No.1, pp.64-72, 2011

[31] Cortes, Patricio, Alan Wilson, Samir Kouro, Jose Rodriguez, and Haitham Abu-Rub, "Model predictive control of multilevel cascaded H-bridge inverters", IEEE Transactions on Industrial Electronics, Vol.57, No.8, pp.2691-2699, 2010

[32] Jain, Bhavna, Shailendra Jain, and R. K. Nema, "Control strategies of grid interfaced wind energy conversion system: An overview", An International Journal of Renewable and Sustainable Energy Reviews, Vol.47, pp.983-996, 2015

[33] Dai, Jingya, Dewei Xu, and Bin Wu, "A novel control scheme for current-source-converter-based PMSG wind energy conversion systems", IEEE Transactions on Power Electronics, Vol.24, No.4, pp.963-972, 2009

[34] Has sanien, Aboul Ella, Tarek Gaber, Usama Mokhtar, and Hesham Hefny, "An improved moth flame optimization algorithm based on rough sets for tomato diseases detection", An International Journal of Computers and Electronics in Agriculture, Vol.136, pp.86-96, 2017

[35] Ramirez, Maria Cleofe Valverde, Haroldo Fraga de Campos Velho, and Nelson Jesus Ferreira, "Artificial neural network technique for rainfall forecasting applied to the Sao Paulo region", An International Journal of hydrology, Vol.301, No.1, pp.146-162, 2005

[36] Taghizadeh, H., and M. Tarafdar Hagh, "Harmonic elimination of cascade multilevel inverters with nonequal DC sources using particle swarm optimization", IEEE Transactions on Industrial Electronics, Vol.57, No.11, pp.3678-3684, 2010